

Evaluation of MODIS data potential to infer water stress for wheat NPP estimation

N.R. PATEL*, V.K. DADHWAL, S.K. SAHA, A. GARG & N. SHARMA

Indian Institute of Remote Sensing, NRSC, ISRO, Dehradun 248 001, India

Abstract: The present, study carried out in Haryana, explores potential of MODIS data for scaling constant light use efficiency (ϵ^*) for computing the net primary productivity (NPP) of wheat crop following Monteith's concept. We compared three scaling approaches ϵ^* in time and space by using three different MODIS derived surface wetness indices, i.e. vegetation temperature condition index (VTCI), water deficit index (WDI) and land surface wetness index (LSWI). The approach using MODIS observations allows estimation of temporal evolution and geographical distribution of NPP of wheat in Haryana. High levels of seasonal NPP in wheat were observed in northern districts of Kaithal, Kurushretra and Fatehabad compared to districts in southern and western Haryana. Among three water stress scalars, the seasonal NPP simulated with LUE (LSWI) was higher in the magnitude (950-1200 g DM m⁻²) and mean NPP (1030 g DM m⁻²). Further, simulated NPP of wheat with LUE (LSWI) had good agreement with observed crop NPP of wheat ($R^2=0.39$, RMSE=64.9 g DM m⁻²) compared to simulated NPP with LUE (VTCI) and LUE (WDI). Statistical analysis revealed that the dynamics and magnitude of absorbed photosynthetically active radiation (APAR) over wheat growing season mainly determined the spatio-temporal dynamics of NPP. The LUE estimates from LWSI were within range of experimental LUE of wheat but did not show significant differences that cause variability in NPP.

Resumen: El presente estudio, llevado a cabo en Haryana, explora el potencial de los datos MODIS para transformar a otras escalas la eficiencia de uso de luz constante (ϵ^*) para el cálculo de la productividad primaria neta (PPN) del trigo a partir del concepto de Monteith. Comparamos tres enfoques para el escalado de ϵ^* en tiempo y espacio por medio del uso de tres diferentes índices de humedad de la superficie derivados de MODIS (con sus siglas en inglés): el índice de la condición térmica de la vegetación (VTCI), el índice de déficit hídrico (WDI) y el índice de humedad de la superficie terrestre (LSWI). El enfoque basado en las observaciones MODIS permite estimar la evolución temporal y la distribución geográfica de la PPN del trigo en Haryana. Se observaron niveles altos de PPN estacional en el trigo en los distritos norteros de Kaithal, Kurushretra y Fatehabad, en comparación con los distritos en el sur y occidente de Haryana. Entre tres escalares de estrés hídrico, la PPN estacional simulada con LUE (LSWI) fue mayor en el intervalo de la PPN (950-1200 g DM/m²) y en su valor medio (1030 g DM/m²). Además, la PPN simulada de trigo con LUE (LSWI) tuvo una concordancia buena con la PPN observada de la cosecha de trigo ($R^2=0.39$, RMSE=64.9 g DM m⁻²), en comparación con la PPN simulada con LUE (VTCI) y LUE (WDI). El análisis estadístico reveló que la dinámica y la magnitud de la radiación fotosintéticamente activa absorbida (RFAA) a través de la temporada de crecimiento del trigo determinaron principalmente la dinámica espacio-temporal de la PPN. Las estimaciones de LUE a partir del LWSI estuvieron dentro del intervalo del LUE experimental del trigo, pero no mostraron diferencias significativas capaces de causar variabilidad en la PPN.

* Corresponding Author; e-mail: nrpatel@iirs.gov.in

Resumo: O presente estudo, realizado em Haryana, explora o potencial de dados do MODIS para a graduação da constante de eficiência do uso da luz (ϵ^*) para calcular a produtividade primária líquida (NPP) da cultura de trigo de acordo com o conceito de Monteith. Compararam-se três abordagens de graduação de ϵ^* , no tempo e no espaço, usando três índices MODIS diferentes derivados do índice de superfície húmida i.e. índice da condição de temperatura da vegetação (VTCI), índice do deficit hídrico (WDI) e índice de humidade da superfície do solo (LSWI). A aproximação que usa as observações do MODIS permite a estimação da evolução temporal e a distribuição geográfica da NPP do trigo em Haryana. Os elevados níveis sazonais da NPP no trigo foram observados em distritos do norte de Kaithal, de Kurushretra e de Fatehabad comparados aos distritos do sul e a ocidente em Haryana. Entre os três valores do stress hídrico, a NPP sazonais, simuladas com LUE (LSWI), era a mais elevada (950-1200 g DM/m²) com um valor médio de NPP de 1030 g DM/m². Além disso, o valor de NPP simulado do trigo com LUE (LSWI) era convergente com o valor observado de NPP obtido em condições de cultura ($R^2=0.39$, RMSE=64.9 g DM m⁻²) comparado com o valor simulado de NPP com o LUE (VTCI) e o LUE (WDI). A análise estatística revelou que a dinâmica e o valor da radiação fotossintética activa absorvida na estação de crescimento do trigo (APAR) determinaram, principalmente, a dinâmica espaço-temporal da NPP. As estimativas de LUE a partir de LWSI encontravam-se dentro do intervalo experimental de LUE para o trigo mas não mostravam diferenças significativas que justificassem a variabilidade da NPP.

Key words: Light use efficiency, MODIS, net primary productivity, water stress, wheat.

Introduction

Net primary productivity (NPP) is an important biophysical component of the ecosystem function and plays an important role in analyzing carbon balance and spatio-temporal distribution of CO₂. Remotely sensed data from sensors such as Moderate Resolution Imaging Spectroradiometer (MODIS) are useful for monitoring the productivity from regional to global scales (Yuan *et al.* 2006) because reflectance can be converted into biophysically meaningful descriptors of the land surface, including net primary productivity (NPP). NPP represents the amount of new carbon stored as biomass in various plant parts and is a quantitative measure of plant growth and carbon uptake (Waring & Running 1998). NPP is related to photosynthetic activity and can be estimated from remotely sensed data by observing the patterns of light absorption (Sellers *et al.* 1995). Remote sensing techniques have, therefore, naturally emerged as the primary source for deriving large-area NPP information.

Monteith (1972 & 1977) proposed light use efficiency (LUE) concept, which represents the primary productivity as product of absorbed

photosynthetically active radiation (APAR) and constant light use efficiency (ϵ^*). Early LUE approaches assumed constant ϵ^* until it was found that ϵ^* varies between and within vegetation types. These variations may be attributed to variable temperature and water situations, which cause reduction in the LUE, especially in arid and semi-arid environments (Bradford *et al.* 2005; Nouvellon *et al.* 2000; Ruimy *et al.* 1994). LUE models such as GLO-PEM (Prince & Goward 1995) and Carnegie-Ames-Stanford-Approach (CASA) (Field *et al.* 1995; Potter *et al.* 1993) take into account the down-regulators of constant ϵ^* in the form of environmental stressors (both temperature and water) derived from meteorological measurements. In the CASA model, the water stress scalar (W_s) is represented as relative soil moisture deficit determined using a simple one-layer bucket model. Some studies have also focused on deriving canopy water stress by using satellite observations in optical and infrared regions (Jackson 1982; Moran *et al.* 1994; Sandholt *et al.* 2002; Xiao *et al.* 2002). The majority of these studies used optical and thermal infrared (TIR) data to generate an index as a proxy of water stress ($W_s=1-ET/ET_m$) and is defined as a function of the ratio between actual

and potential evaporation rates on the earth surface. The TIR data is linked to evaporative cooling and thus, linked to soil moisture and water stress, whereas the shortwave infrared (SWIR) is sensitive to canopy water content and the indices derived from SWIR and near infrared (NIR) wavelengths have been found to be sensitive to water stress (Fensholt & Sandholt 2003). A few studies have demonstrated the use of stress indices derived either from TIR (Sandholt *et al.* 2002; Moran *et al.* 1994) or SWIR (Xiao *et al.* 2005) bands as a measure of W_s in biospheric NPP models and found that the inclusion of a water stress parameter directly from satellite improves accuracy of NPP modeling.

The MODIS, onboard Terra and Aqua satellites, provides observations in 36 spectral bands covering visible (459-479 nm, 545-565 nm, 620-670 nm), NIR (841-875 nm, 1230-1250 nm), SWIR (1628-1652 nm, 2105-2155 nm) and TIR bands at spatial resolution ranging from 250 m to 1 km. The availability of a diverse range of observations by MODIS offers ample scope for deriving information on key variables of NPP models such as fPAR and water stress scalars. The present study was carried out with two objectives: (i) comparison of scaling LUE by using water stress scalars derived from different remote sensing methods, (ii) estimation of the primary productivity of wheat in Haryana state of India by LUE approach with down-regulators.

Materials and methods

Study area

Haryana (27° 39' - 30° 55' N and 74° 27' - 77° 36' E) is an agrarian state of India (Fig. 1). Geologically, Haryana has been divided into three zones: the Shiwalik hills, Aravali hills and Indo-Gangetic alluvial plain. Nearly 97% of the state lies in Indo-Gangetic alluvial plain. The land is generally flat, covered with loamy soil and highly suitable for agriculture. Annual rainfall in this state varies from more than 1000 mm in hilly tracts to less than 300 mm in the south-western districts *viz.*, Bhiwani, Hisar and Sirsa Districts (Dahiya *et al.* 1988). The annual evapotranspiration of the region is quite high and exceeds 1200 mm all over the state. The rainfall received during *Rabi* season (December-March) also varies across the state with high rainfall in northern districts *viz.*, Kurukshetra, Ambala,

Kaithal as compared to southwestern districts *viz.*, Bhiwani, Mahendragarh and Hisar. Food grain crops account for 72.4% of the total cropped area, of which wheat occupies 42.7%, rice 14%, pearl millet 19.3%, pulses 17.4%, and others 13.5%.

Data

We used 8-day composites of surface reflectance at two resolutions, 250 m and 500 m, and land surface temperature at 1km resolution. The moderate resolution (250 m) level-3 product (MOD09Q1) was used to derive the fraction of absorbed photosynthetically active radiation (fPAR). The 8-day composite of the seven-band surface reflectance (MOD09A1) formed the basic input for deriving the water stress scalar. The MOD09 products were corrected for the effects of atmospheric gases, thin cirrus clouds and aerosols (Vermote & Vermeulen 1999). The MODIS product also included information on cloud interference. The other satellite input was MODIS level-3 land surface temperature (MOD11A2) as a composite of daily land surface temperature derived using split-window algorithms. These satellite data were created by the MODIS land discipline team (<http://modis-land.gsfc.nasa.gov>) and distributed to users freely through EOS Data Gateway (<http://edcimswww.cr.usgs.gov/pub/imswelcome>). The 8-day composite images of above data at 250 m, 500 m and 1 km resolution were acquired for the period from 25th November, 2003 to 6th April, 2004, which matched with the growing season of wheat during year 2003-04.

Meteorological variables were collected for the period of entire growing season of wheat, particularly daily maximum and minimum temperatures recorded over 10 stations falling in Haryana and its surroundings. In the present study, distribution of the wheat crop during 2003-04 was obtained from major crops classified from AWiFS (Advance Wide-Field Sensor) data (Patel *et al.* 2007). Ground-based crop yield and acreage of wheat crop in the same season were taken from Bureau of Economic Survey (BES) for validation of results.

NPP model

In the LUE approach (Monteith 1972 & 1977), NPP is taken as the product of PAR absorbed by the vegetation canopy and LUE:

$$\text{NPP} = \text{APAR} \times \text{LUE} \quad (1)$$

where, NPP is net primary productivity (g Dry mass (DM) m⁻² time⁻¹), APAR is the absorbed

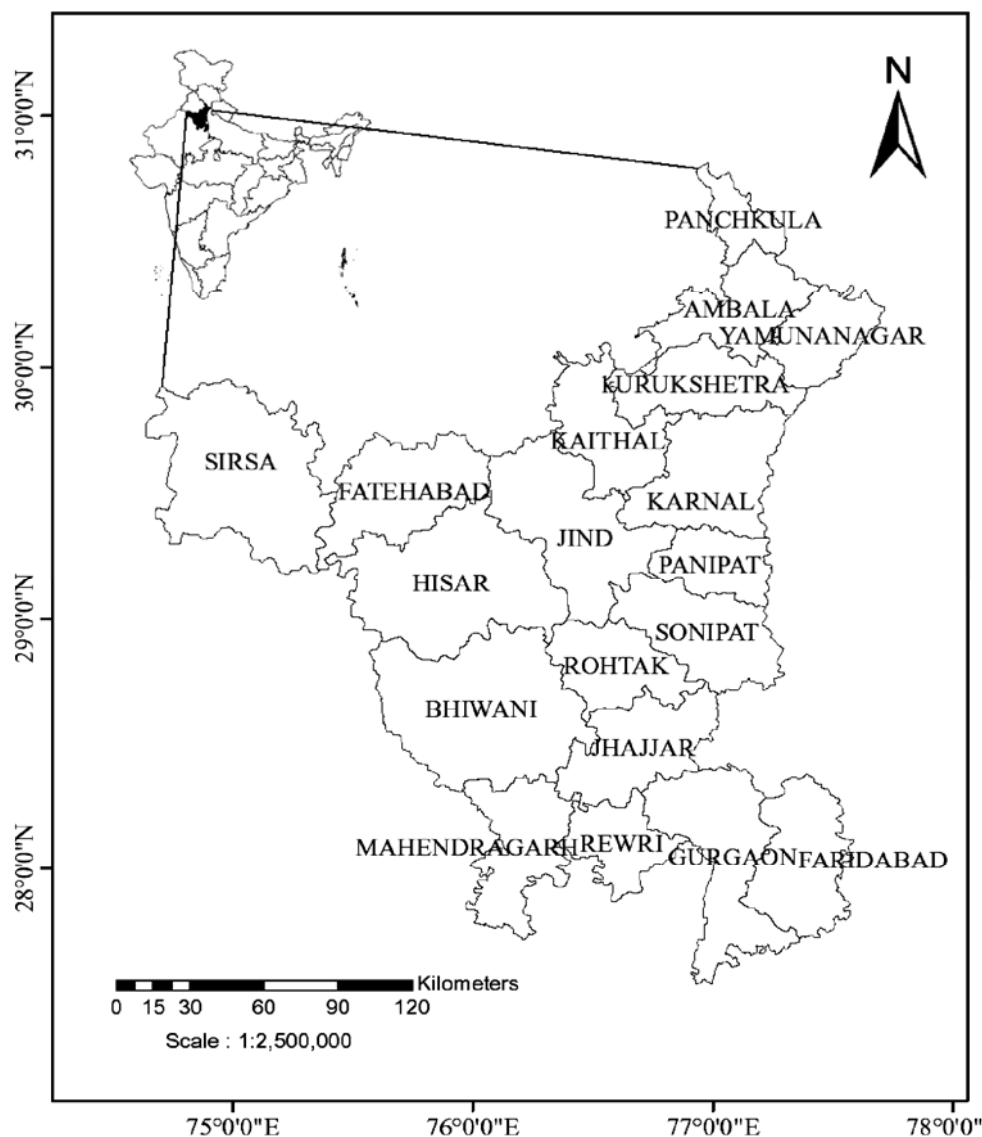


Fig. 1. Study area with district boundaries.

photosynthetically active radiation ($\text{MJ m}^{-2} \text{ time}^{-1}$) and LUE is the light use efficiency (g MJ^{-1}). The APAR itself is a product of incident photosynthetically active radiation (PAR) and the fraction of absorbed PAR (fPAR) which is easily quantifiable from remote sensing. The fPAR in general had strong linear relationships with NDVI and was derived either by using vegetation specific regression constants of such relationship (Potter *et al.* 1993; Prince & Goward 1995) or linear scaling based on NDVI (Sellers *et al.* 1996). In the present study, fPAR was quantified from NDVI as:

$$\text{fPAR} = \frac{(\text{NDVI}_{\text{max}} - \text{NDVI}_{\text{min}}) (\text{fPAR}_{\text{max}} - \text{fPAR}_{\text{min}})}{(\text{NDVI}_{\text{max}} - \text{NDVI}_{\text{min}}) + \text{fPAR}_{\text{min}}} \quad (2)$$

where, NDVI_{max} and NDVI_{min} are defined as 98th and 2nd percentiles, respectively of maximum and minimum NDVI of wheat during its growth cycle. fPAR_{min} and fPAR_{max} are set equal to 0.01 and 0.95, which represents the extremes of potential canopy absorption of PAR (Los *et al.* 2000; Sellers *et al.* 1996). The maps of fPAR thus, obtained at 8-day interval were later multiplied with corresponding interpolated surfaces of incident PAR for estimating APAR for the same

interval. The daily incident PAR as a fraction of the incoming solar radiation was calculated using Bristow & Campbell (1984) model.

Down-regulation of maximum LUE

LUE varies spatially across vegetation types and temporally within individual plant or biome types due to variable temperature and moisture conditions. An assumption of constant LUE in NPP estimation is unrealistic. We therefore, down-regulated the maximum LUE during times of moisture and temperature stress. The LUE thus was determined using following equation (Xiao *et al.* 2005):

$$LUE = \varepsilon^* T_s W_s \quad (3)$$

where, ε^* is maximum light use efficiency of wheat, 2.8 g/MJ PAR (Fischer 1983; Garacia *et al.* 1988; Khan 2000), and T_s and W_s are temperature and water stress scalars, respectively. The T_s is estimated at each time step, using the equation developed for the terrestrial ecosystem model (Raich *et al.* 1991):

$$T_s = \frac{(T - T_{\min})(T - T_{\max})}{[(T - T_{\min})(T - T_{\max})] - (T - T_{\text{opt}})^2} \quad (4)$$

where, T is the interpolated surface of mean monthly temperatures from stations, T_{\min} , T_{\max} , and T_{opt} are minimum, maximum, and optimal temperature for photosynthetic activities, respectively. For wheat, we used 5.0, 35.0 and 22.0 °C for T_{\min} , T_{\max} , and T_{opt} , respectively (Porter & Gawith 1999).

Over the last two decades, several remote sensing techniques have been used to infer water stress as a function of relative evapotranspiration deficit. In the present study, we chose three formulations as a proxy for the W_s factor: vegetation temperature condition index (VTCI, Wan *et al.* 2004), water deficit index (Moran *et al.* 1994), and land surface wetness index (Xiao *et al.* 2002).

Vegetation temperature condition index

The vegetation temperature condition index (VTCI) is an index derived by parameterization of LST verses NDVI scatter plot for each 8-day interval of MODIS data used in the study. It is defined as the ratio of LST differences among pixels with a specific NDVI value in a sufficiently large study area. The value of VTCI ranges from 0 to 1. Lower values of VTCI represent lower evapotranspiration rates (ET). Mathematically, the water stress scalar from VTCI is written as:

$$VTCI = (ET/ET_m) = \frac{LST_{\max} - LST}{LST_{\max} - LST_{\min}} \quad (5)$$

where, $LST_{\max} = a + b \times NDVI$, $LST_{\min} = a' + b' \times NDVI$

The LST_{\max} and LST_{\min} are maximum and minimum LSTs of pixels, which have same NDVI values in a study region, respectively and LST denotes the observed actual LST value of pixels. Coefficient a , b , a' and b' were computed from LST verses NDVI scatter plot. for every 8-day interval. The LST_{\max} and LST_{\min} represent “dry” and “cold” edges, respectively. The slope and intercept term of these edges were obtained by simple least square regression.

Water deficit index

The water deficit index (WDI) quantifies the relative rate of latent heat flux leaving a surface by evaporation and transpiration, where the surface is a mixture of vegetation and bare soil. The WDI is defined as 0.0 for well-watered conditions (i.e., a completely wet surface, where latent heat flux is limited only by atmospheric demand) and 1.0 for no available water (i.e., a completely dry surface where there is no loss of water or little evapotranspiration). Recently, Verstraeten *et al.* (2006) has formulated WDI based on a triangle formed by surface-air temperature differential (ΔLST) and vegetation index. Mathematically WDI from $\Delta LST/NDVI$ triangle can be expressed as:

$$WDI = 1 - \frac{ET}{ET_m} \approx \frac{\Delta LST_{\min} - \Delta LST_0}{\Delta LST_{\min} - \Delta LST_{\max}} \approx \frac{a_{\min} NDVI + b_{\min} - \Delta LST_0}{(a_{\min} - a_{\max}) NDVI + (b_{\min} - b_{\max})} \quad (6)$$

where, ΔLST_0 denotes the difference between the LST and ambient air temperature. ΔLST_{\min} and ΔLST_{\max} denotes maximum and minimum evapotranspiration lines, respectively, and represented as regression lines such as $\Delta LST_{\min} = a_{\min} \times NDVI + b_{\min}$ and $\Delta LST_{\max} = a_{\max} \times NDVI + b_{\max}$. The coefficients such as a_{\min} , a_{\max} , b_{\min} , and b_{\max} were computed from ΔLST_0 verses NDVI scatter plot for each 8-day interval.

Land surface wetness index

The land surface wetness index (LSWI) is linear combination of NIR and SWIR bands and calculated as:

$$LSWI = \frac{\delta_{NIR} - \delta_{SWIR}}{\delta_{NIR} + \delta_{SWIR}} \quad (7)$$

where, δ_{NIR} and δ_{SWIR} are reflectance in NIR (841-875 nm) and SWIR (1628-1652 nm) regions, respectively, for each 8-day composite of MODIS data. We used $LSWI$ to estimate seasonal dynamics of the water stress scalar (W_s) based on the simple approach of Xiao *et al.* (2005):

$$W_s = \frac{1 + LSWI}{1 - LSWI_{max}} \quad (8)$$

where, $LSWI_{max}$ is the maximum $LSWI$ within the wheat growing season for individual pixels.

Approach

The NPP of wheat for each 8-day interval corresponding to MODIS composite imagery was primarily estimated at the pixel level as a product of

canopy during the same time period. The conversion of APAR into NPP for each time step i was established with a temporally variant light use efficiency obtained by reducing ϵ^* by water and temperature stress scalars (Eq.3). The methodology depicted in Fig. 2.

The 8-day composites of surface reflectance products (MOD09Q1) covering the entire wheat growing season (25th November to 6th April, 2004) were first reprojected to Alber's equal area projection with spheroid and datum as WGS 84. Time series of normalized difference vegetation index (NDVI) were derived from these surface reflectance and converted into the fraction of absorbed photosynthetically active radiation (fPAR) by equation (2). Since no measurements were available for incoming solar radiation, the Bristow & Campbell (1984) formulation based on temperature was used to obtain daily estimates of

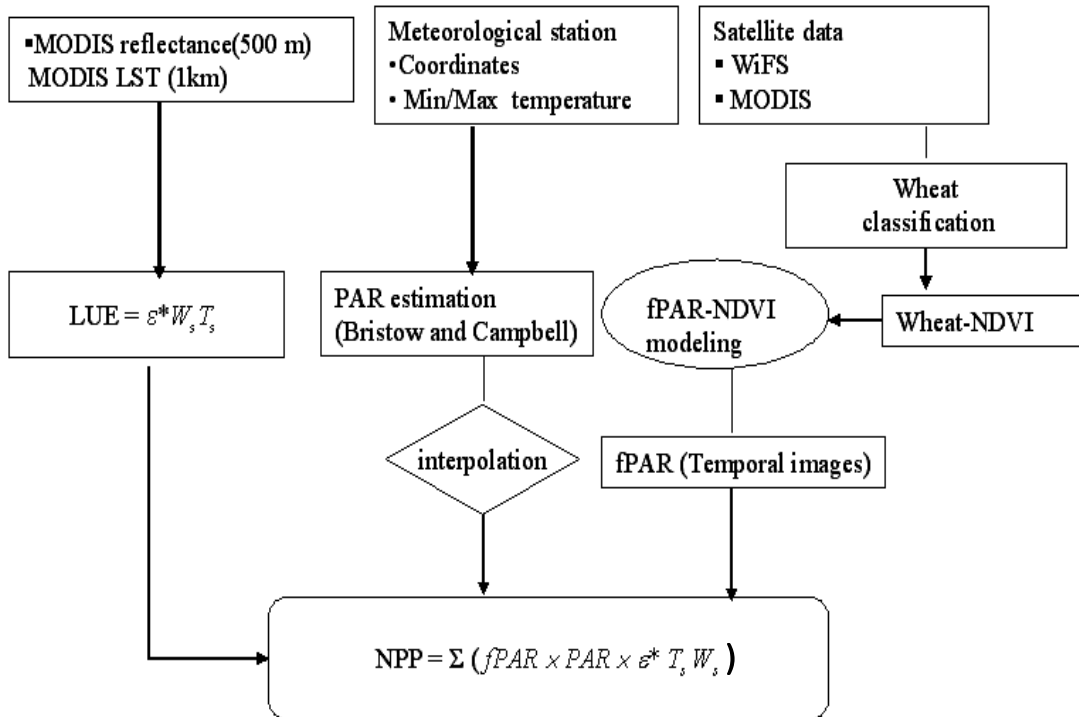


Fig. 2. The steps involved in the estimation of NPP (schematic).

absorbed PAR (APAR) and light use efficiency estimates obtained from down-regulation of maximum LUE of C3 crops (i.e. 2.8 g MJ⁻¹). The APAR for every 8-day interval was estimated as a product of incident PAR and the fraction of photosynthetically active radiation (fPAR) by the

solar radiation. The empirical constants of the Bristow and Campbell model were parameterized for Hisar district (Patel *et al.* 2007) and used for all stations falling in Haryana. The estimates of solar radiation over 10 stations were later subjected to Inverse Distance Weighted interpolation in order

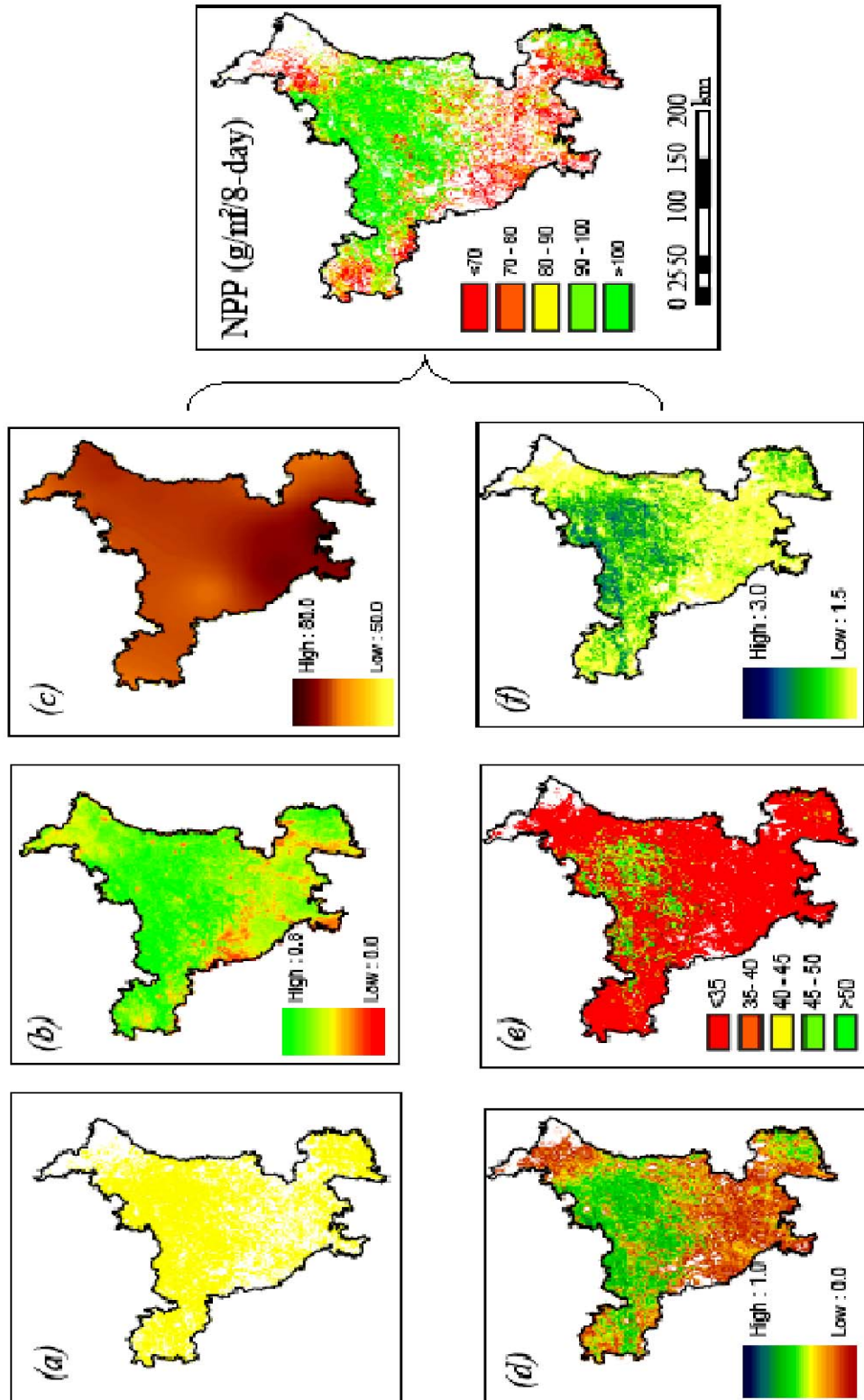


Fig. 3. Components of NPP modelling from satellites and climatic data (period 6-13 March, 2004): (a) location of wheat crop areas, (b) NDVI from MODIS, (c) Interpolated PAR from weather stations, (d) Absorbed PAR (APAR=fPAR \times PAR) and (f) down-regulated light use efficiency.

to obtain solar radiation for MODIS pixel resolution. Incident PAR was approximated as 45 percent of incoming solar radiation. Similarly, the maximum and minimum daily air temperatures were interpolated and converted to an 8-day average in a 1-km grid. Crop yield data at the district level was converted to seasonal NPP of wheat by using a harvest index (0.35) and moisture content.

Results and discussion

Spatial pattern of NPP components

Spatial variation, in different intermediate components of the NPP model, were analyzed for the post-anthesis stage of 6-13 March, 2004 (Fig. 3). The NDVI as a measure of fPAR ranged from 0.18 to 0.78 with the highest values observed in northern part of state. The PAR shows large spatial variation with higher PAR in south-bound areas compared to north-bound areas. Despite high PAR in the southern part of area, absorbed PAR was relatively low ($<35 \text{ MJ m}^{-2}$) due to less vegetation cover as depicted in the NDVI image. The higher APAR (range $45\text{-}55 \text{ MJ m}^{-2}$) was mainly observed in the northern area with better crop cover conditions, particularly during this post-anthesis stage. A wide range of variation in APAR could be much more related to crop cover percentage than variability in incident PAR over space. According to equation (3), the light use efficiency varied between 1.85 and 2.72 g MJ^{-2} depending upon spatial variation in soil moisture and environmental factors. The LUE remained lower than potential or maximum LUE observed for wheat under optimal crop growing environment. The biomass productivity in terms of NPP for the given 8-day period ranges from 57.6 g m^{-2} to 165.8 g m^{-2} . Such large geographical variation in productivity for irrigated wheat crop of Haryana mainly arose from differences in absorbed PAR. It seems that LUE has little influence on NPP in irrigated wheat crop.

Seasonal dynamics of NPP and light use efficiency

The LUE model was implemented with environmental regulators at 8-day intervals to estimate the temporal pattern of NPP. The resultant seasonal dynamics of NPP using three water scalars are presented together with NDVI for Hisar District (Fig. 4). During the early part of

the wheat growing season, i.e. DOY 333 to 357 of 2003, both NPP and NDVI stood at very low levels due to less photosynthetic activity in the absence of canopy cover. From DOY 1 of 2004, despite NDVI increasing suddenly, NPP only gradually increased until DOY 25 due to reduced temperature and PAR in January because temperature below thresholds limited photosynthesis activity. The NPP showed a lag behind NDVI and attained its peak at post-anthesis stage between DOY 57 and 65 of 2004. The DOY 65 onwards, both the NPP and NDVI declined in similar fashion on account of senescence as the crop reached to maturity or harvest. Among the NPP simulated with different water scalars, the NPP by using the water scalar (W_s) from *LSWI* remained higher during the active crop growth period (i.e. DOY 33 to 81 of 2004) than those of W_s (*VTCD*) and W_s (*WDI*). These differences in simulated NPP were mainly explained by variation in light use efficiencies resulted from different water scalars (Fig. 5). Higher light use efficiency from W_s (*LSWI*) led to high levels of NPP during period of maximum growth accumulation. Furthermore, LUE from W_s (*LSWI*) was found in close agreement with experimentally observed LUE at Hisar (Sharma *et al.* 2000). These results also revealed that *LSWI* correctly captured water stress effects and down-regulated maximum LUE (ϵ^*) within the range (2.0–2.8 g/MJ PAR) of experimentally observed LUE of wheat during the period (DOY 33-89 of 2004). The large difference in LUE (*LSWI*) from observed values during the early phase of wheat growth was mainly due to less sensitivity of *SWIR* wavelength to canopy water content/water stress when canopy cover is sparse ($\text{NDVI} < 0.4$).

Spatial pattern of NPP

The NPP simulated at 8-day interval was summed over the wheat growing season (Fig. 6). A wide range of variation existed across different parts of Haryana. In general, high levels of NPP were observed in Kaithal, Kurushretra and Fatehabad compared to Bhiwani, Mahendragarh, Rewari and Sirsa in southern and western Haryana. Results also revealed comparatively high seasonal NPP of wheat over entire wheat growing areas when simulated with light use efficiency derived using *LSWI* as water stress scalar. Whereas seasonal NPP estimates obtained with water *VTCD* and *WDI* as stress scalars were quite low.

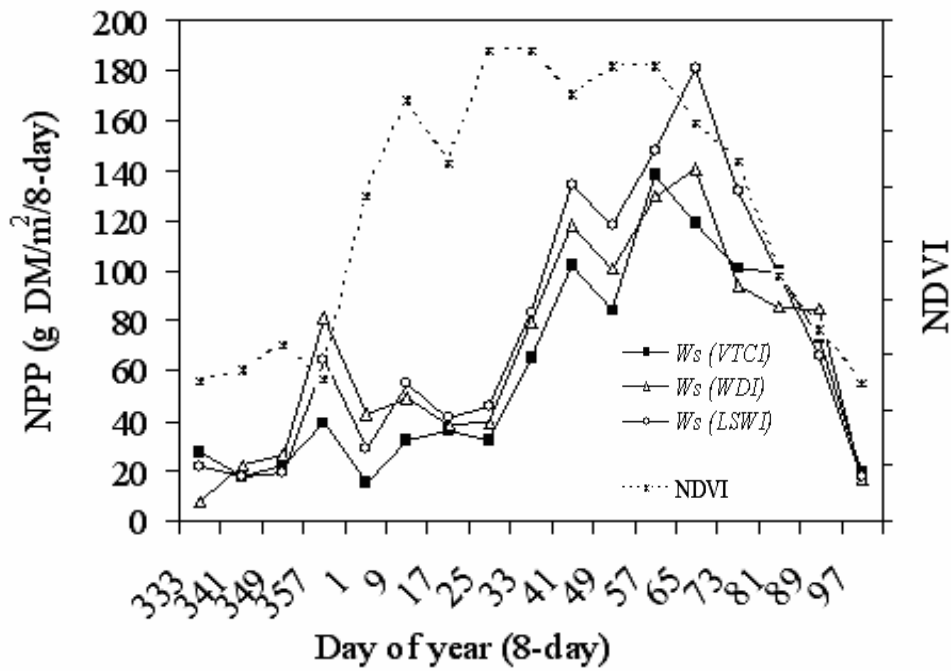


Fig. 4. Temporal dynamics of net primary productivity (NPP) of wheat (Hisar District, India; 29° 10' N, 75° 45' E).

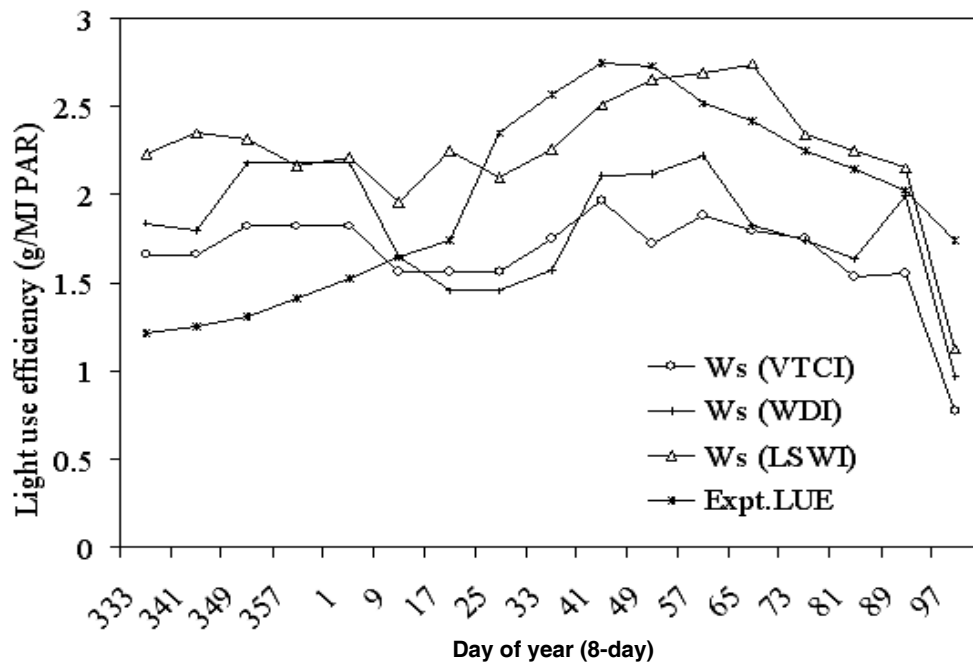


Fig. 5. Comparison of the adjusted light use efficiency from different water stress scalars and experimental LUE.

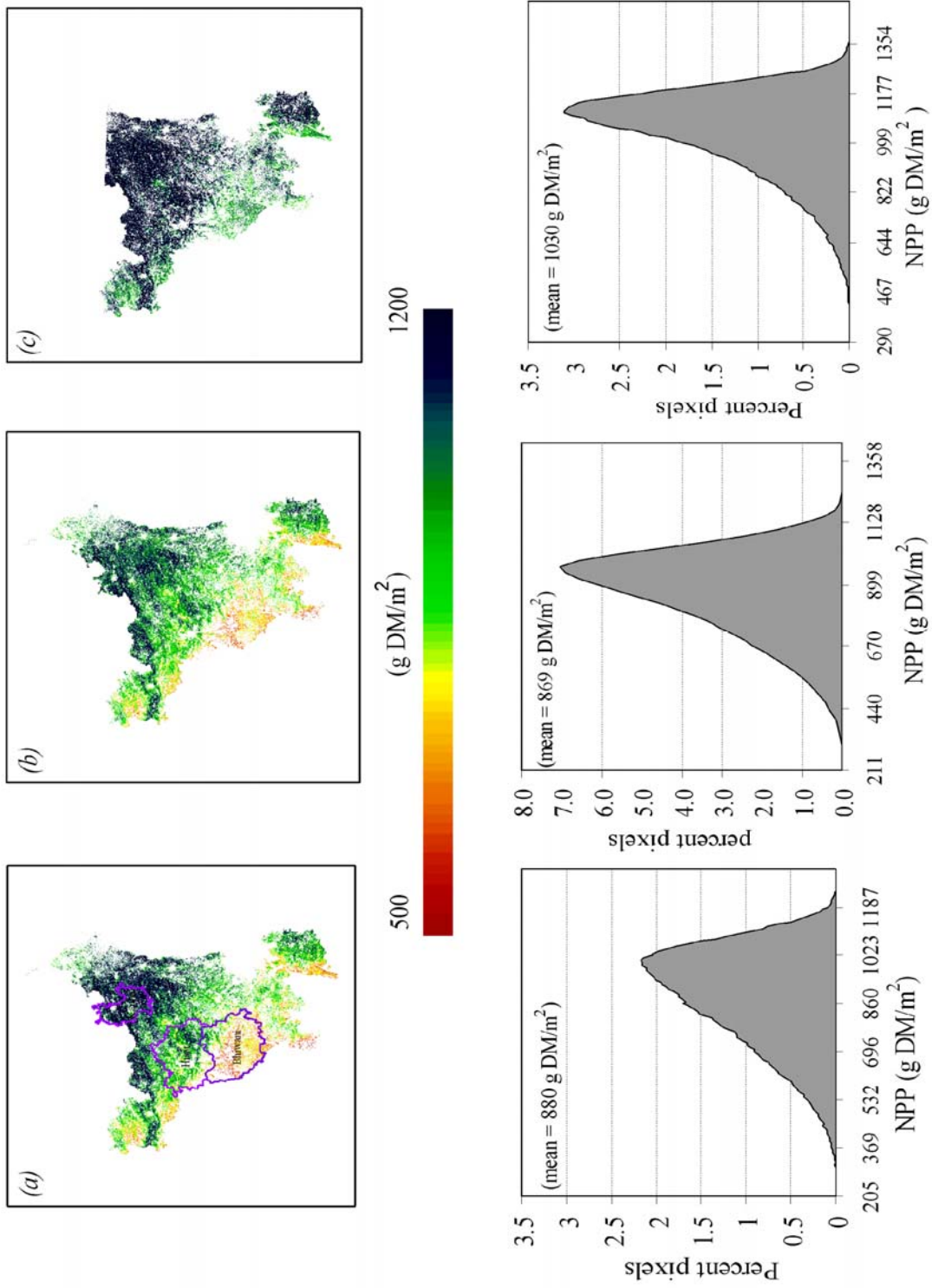


Fig. 6. Spatial pattern with histogram frequency of NPP of wheat crop for different water stress scalars: (a) LUE (VTCI), (b) LUE (WDD) and (c) LUE (LSWI). Frequency plot shown beneath the each map.

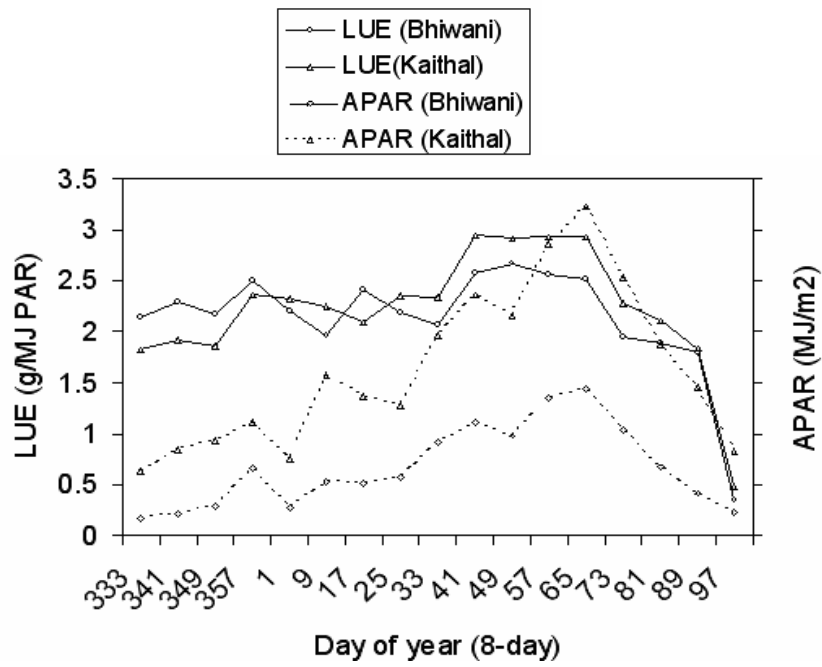


Fig. 7. Temporal pattern of APAR and LUE over Kaithal and Bhiwani districts in India. LUE values depicted were calculated using the LSWI water stress scalar.

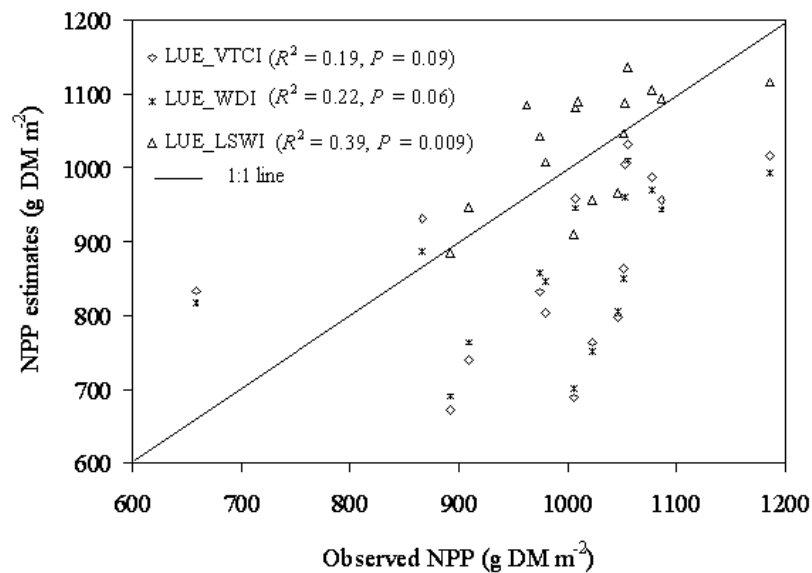


Fig. 8. Comparison of simulated and observed NPP of wheat crop in Haryana (Ambala, Panchkula and Yamunanagar districts were not considered).

Spatial distribution of NPP from LUE (LSWI) had a maximum frequency in the range of 950 to 1200 g DM m⁻² and mean NPP equaled 1030 g DM m⁻² (Fig. 6), while the mean seasonal NPP of wheat obtained with LUE (VTCI) and LUE (WDI) were 880 g DM m⁻² and 869 g DM m⁻², respectively. Spatial variation in NPP over different districts was mainly controlled by dynamics of absorbed PAR (APAR), as illustrated in Kaithal and Bhiwani districts (Fig. 7). Comparatively higher NPP in Kaithal than Bhiwani was found due to high levels of APAR throughout growing season of wheat. The Wilcoxon test (Wilcoxon statistic=0.0, $p < 0.0001$) and positive mean bias (+19.3 MJ m⁻² APAR) explained the tendency of APAR in Kaithal to be greater than that of Bhiwani. Light use efficiency also varied between two regions, particularly during the period of maximum growth accumulation however, its contribution in determining NPP was relatively low. The probability of wilcoxon test for LUE in Kaithal to be greater than that of Bhiwani is non-significant (Wilcoxon statistic=52.5, $p = 0.14$) but positive value of mean bias (+0.1) reflects the contribution of LUE in causing differences in NPP.

Comparison of simulated and ground-based NPP

Seasonal NPP of wheat compared against ground-based crop NPP estimates obtained from crop statistics at district level revealed that LUE (LSWI) provided satisfactory estimates of seasonal NPP of wheat in Haryana (Fig. 8). Relative deviation between simulated and observed crop NPP was within range of $\pm 10\%$ for LUE based on *LSWI*. The magnitude of relative deviation with LUE (VTCI) and LUE (WDI) were quite large ($> \pm 15\%$) for majority of districts in Haryana. A close relationship was observed between simulated NPP from LUE (LSWI) and ground based crop NPP ($R^2 = 0.39$). The Root Mean Square Error (RMSE) associated with seasonal NPP estimates of wheat with LUE (LSWI) is 64.9 g DM m⁻² which was less than 10% of mean observed crop NPP. The other two methods i.e., LUE (VTCI) and LUE (WDI) showed relatively higher RMSE of 111.0 and 108.0 g DM m⁻², respectively.

Conclusions

Results showed that the SWIR band of MODIS had good success in deriving water stress as down-

regulator of maximum light use efficiency (ϵ^*) of wheat and presumably other C₃ crops for NPP modeling. Light use efficiency of wheat obtained with water stress scalars by different approaches varied both spatially and temporally. Amongst three approaches, reducing maximum LUE with *LSWI* captured the trend observed in LUE of wheat experimentally over Hisar District. While two other approaches (*VTCI*, *WDI*) based on Ts/NDVI space failed to represent temporal variation in LUE due to their limited sensitivity to moisture stress when canopy cover is full. NPP estimates of wheat obtained from LUE based on *LSWI* showed good agreement with observed NPP of wheat in Haryana.

References

- Bradford, J.B., J.A. Hicke & W.K. Lauenroth. 2005. The relative importance of light-use efficiency modifications from environmental conditions and cultivation for estimation of large-scale net primary productivity. *Remote Sensing of Environment* **96**: 246-255.
- Bristow, K. & G.S. Campbell. 1984. On the relationship between incoming solar radiation and daily maximum and minimum temperature. *Agricultural & Forest Meteorology* **31**: 159-166.
- Dahiya, I. S., M. Singh, A.V. Shanwal, M.S. Kuhad & S.P.S. Karwasra. 1988. *Land Resources and Land Use planning in Haryana*. Directorate of Research, Haryana Agricultural University, Hisar, India.
- Fensholt, R. & I. Sandholt. 2003. Derivation of a shortwave infrared water stress index from MODIS near- and short wave infrared data in a semi-arid environment. *Remote Sensing of Environment* **87**:111-121.
- Field, C.B., J.T. Randerson & C.M. Malmstrom. 1995. Global net primary production combining ecology and remote-sensing. *Remote Sensing of Environment* **51**: 74-88.
- Fischer, R.A. 1983. Wheat. pp. 129-154. In: W.H. Smith & S.J. Banta (eds.) *Potential Productivity of Field Crops Under Different Conditions*. International Rice Research Institute, Los Banos, Philippines.
- Garcia, R., E.T. Kanemasu, B.L. Blad, A.A. Bauer, J.L. Hatfield, D. Major, R.J. Reginato & K.G. Hubbard. 1988. Interception and use efficiency of light in winter wheat under different nitrogen regimes. *Agricultural & Forest Meteorology* **44**: 175-186.
- Jackson, R.D. 1982. Canopy temperature and crop water stress. *Advances in Irrigation* **1**: 43-85.

- Khan, N.A. 2000. *Simulation of Wheat Growth and Yield Under Variable Sowing Date and Seeding Rate*. M.Sc. Thesis, Department of Agronomy, University of Agriculture, Faisalabad, Pakistan.
- Los, S.O., G.J. Collatz, P. J. Sellers, C.M. Malmstrom, N.H. Pollack, R S. Defries, L. Bounou, M.T. Parris, C.J. Tucker & D.A. Dazlich. 2000. A global 9-yr biophysical land surface dataset from NOAA AVHRR data. *Journal of Hydrometeorology* **1**: 183-199.
- Monteith, J.L. 1972. Solar radiation and productivity in tropical ecosystems. *Journal of Applied Ecology* **9**:747-766.
- Monteith, J.L. 1977. Climate and the efficiency of crop production in Britain. *Philosophical Transactions of the Royal Society of London* **B281**: 277-294.
- Moran, M.S., T.R. Clarke, Y. Inoue & A. Vidal. 1994. Estimating crop water deficit using the relation between surface-air temperature and spectral vegetation index. *Remote Sensing of Environment* **49**: 246-263.
- Nouvellon, Y., D.L. Seen & S.G. Verma. 2000. Time course of radiation use efficiency in a short - grass ecosystem: consequences for remotely sensed estimation of primary production. *Remote Sensing of Environment* **71**: 43-55.
- Patel, N.R., B. Bhattacharjee, A.J. Mohammed, Tanu Priya & S.K. Saha. 2007. Remote sensing of regional yield assessment of wheat in Haryana, India. *International Journal of Remote Sensing* **27**: 4071-4090.
- Porter, J.R. & M. Gawith. 1999. Temperatures and the growth and development of wheat: a review. *European Journal Agronomy* **10**: 23-36.
- Potter, C.S., J.T. Randerson, C.B. Field, P.A. Matson, P.M. Vitousek, H.A. Mooney & S.A. Klooster. 1993. Terrestrial ecosystem production: a process model-based on global satellite and surface data. *Global Biogeochemical Cycles* **7**: 811-841.
- Prince, S.D. & S.N. Goward. 1995. Global primary production: a remote sensing approach. *Journal of Biogeography* **22**: 815-835.
- Raich, J.W., E.B. Rastetter, J.M. Melillo, D.W. Kicklighter, P.A. Steudler, B.J. Peterson, A.L. Grace, B. Moore & C.J. Vorosmarty. 1991. Potential net primary productivity in South America: application of a global model. *Ecological Applications* **1**:399-429. .
- Ruimy, A., B. Saugier & G. Dedier. 1994. Methodology for the estimation of terrestrial net primary production from remotely sensed data. *Journal of Geophysical Research* **99**: 5263-5283.
- Sandholt, I., K. Rasmussen & J. Andersen. 2002. A simple interpretation of the surface temperature/vegetation index space for assessment of surface moisture status. *Remote Sensing of Environment* **79**: 213-224.
- Sellers, P. J., B.W. Meeson, F.G. Hall, G. Asrar, R.E. Murphy & R.A. Schiffer. 1995. Remote sensing of the land surface for studies of global change: Models-algorithms-experiments. *Remote Sensing of Environment* **51**: 3-26.
- Sellers, P.J., D.A. Randall, C.J. Collatz, J.A. Berry, C.B. Field, D.A. Dazlich, C. Zhang & G.D. Colello. 1996. A revised land surface parameterization (SiB2) for atmospheric GCM's. Part I: Model formulation. *Journal of Climate* **9**: 676-705.
- Sharma, K., Ram Niwas & M. Singh. 2000. Effect of sowing time on radiation use efficiency of wheat cultivars. *Journal of Agrometeorology* **2**: 166-169.
- Vermote, E. F. & A. Vermeulen. 1999. Atmospheric correction algorithm: Spectral reflectances (MOD09), ATBD version 4.0. (http://modis.gsfc.nasa.gov/data/atbd_modis08.pdf).
- Verstraeten, W. W., F. Veroustrate & J. Feyen. 2006. Estimating evapotranspiration of European forests from NOAA-imagery at satellite overpass time: Towards an operational processing chain for integrated optical and thermal sensor data products. *Remote Sensing of Environment* **96**:256-276.
- Xiao, X., S. Boles, J.Y. Liu, D.F. Zhuang & M.L. Liu. 2002. Characterization of forest types in Northeastern China, using multi-temporal SPOT-4 VEGETATION sensor data. *Remote Sensing of Environment* **82**: 335-348.
- Xiao, X.M., Q.Y. Zhang, D. Hollinger, J. Aber & B. Moore. 2005. Modeling gross primary production of an evergreen needleleaf forest using MODIS and climate data. *Ecological Applications* **15**: 954-969.
- Wan, Z., P. Wang & X. Li. 2004. Using MODIS Land surface temperature and normalized difference vegetation index products for monitoring drought in the southern Great Plains, USA. *International Journal of Remote Sensing* **25**: 61-72.
- Waring, R.H. & S.W. Running. 1998. *Forest Ecosystems: Analysis at Multiple Scales*. San Diego, California: Academic Press, Inc.
- Yuan J., Niu Zheng & Wang Chenli. 2006. Vegetation NPP distribution based on MODIS data and CASA model - A case study of northern Hebei Province. *Chinese Geographical Science* **16**: 334-341.